Pion spectra in a hadronic transport model for relativistic heavy ion collisions

Bao-An Li and Wolfgang Bauer
National Superconducting Cyclotron Laboratory and Department of Physics and Astronomy, Michigan State University, East Lansing, Michigan 48824
(Received 27 February 1991)

A set of coupled transport equations for the phase-space distribution functions of nucleons, deltas, and pions is solved with the test particle method to study pion production in relativistic heavy ion collisions. The experimentally observed concave shape of the pion spectra is well reproduced. The mechanism that causes the concave shape of the pion spectra is found to be due to the different contributions of the delta resonance produced during the early and the late stages of the heavy ion collision and due to the energy dependence of the pion and delta absorption cross sections. The dependence of the shape of the pion spectra on beam energy, target and projectile mass, and impact parameter is also studied. An approximate scaling function for the shape parameter of the pion spectra is found.

I. INTRODUCTION

In relativistic nuclear collisions of beam energies around 1 GeV/nucleon, about half of the nucleon-nucleon cross section is inelastic, mainly through pion production. The participant region of heavy ion collisions is therefore mainly composed of nucleons, delta resonances, and pions. Interesting information about the dynamics of nuclear reactions and the equation of state of hot and dense matter can be obtained by studying the properties of the produced pions [1,2]. Moreover, pions also influence the production of other particles such as dileptons and high-energy photons which themselves have been used as probes of the nuclear equation of state [3–5].

Among the properties of pions produced in relativistic heavy ion collisions, the excitation function of the pion multiplicity was first used in an attempt to extract the nuclear equation of state by assuming the discrepancy between the experimental data and the intranuclear-cascade model prediction completely comes from the lack of compression energy in the model [1,6]. More elaborated models like the Boltzmann-Uehling-Uhlenbeck (BUU) transport model [7–9] and the quantum molecular dynamics model (QMD) [10], which include the mean field in addition to the two-body collisions, found that the sensitivity of the pion multiplicity is not so obvious, especially when momentum-dependent forces are taken into account [11]. One therefore has been investigating other global properties of pions like pion flow [12] and pion spectra [13].

Recent experimental results from the DIOGENE Collaboration show that pions have a nonzero flow in the reaction plane associated with the baryon collective flow. However, the cascade model calculation predicts values compatible with zero over the whole range of rapidity [12]. QMD model calculations indicate the presence of pion flow, but predicted values are smaller than the experimental data [14]. The mechanism that produces pion flow is therefore not yet well established.

Some features of the pion kinetic-energy spectrum in relativistic heavy ion collisions are expected to provide information about the space-time dynamics of the reaction. One interesting feature observed is that pion spectra in central heavy ion collisions show a concave shape which can be well fitted by a superposition of two Boltzmann distributions with widely different slope parameters. This phenomenon has been observed in Ar+KCl collisions at a beam energy of 1.8 GeV per nucleon [13] and La+La at $E/A=1.35$ GeV [15]. Preliminary results from Au+Au at $E/A=1.15$ GeV [16] also show this feature. Several possible mechanisms have been proposed to explain this phenomenon [13,15,17,18].

In ultrarelativistic heavy ion collisions and proton-induced reactions, pion transverse momentum spectra also show a concave shape [19]. This has generated much interest, and the origin of this phenomenon has been vigorously debated in the literature [20–24]. Therefore the understanding of the mechanism that causes the concave shape of the pion kinetic-energy spectra in relativistic heavy ion collisions may shed some light on the origin of the concave shape of the pion transverse momentum spectra in ultrarelativistic nuclear collisions [18].

In this context it is also interesting to note that the soft pion enhancement is even seen in $\sqrt{s}=1.8$ TeV $p\bar{p}$ collisions at Fermilab [25].

The above-mentioned situation concerning the study of pion properties strongly calls for a more adequate account of pions in the available relativistic heavy ion collision models.

The BUU transport model for intermediate-energy heavy ion collisions introduced by Bertsch *et al.* [8] and its relativistic extension by Ko *et al.* [26] and Blättel *et al.* [27] is one of the most successful models, in terms of reproducing experimental observables. However, the BUU equation describes the time evolution of the phase-space distribution function for only one kind of particle. The collision integral in this equation was derived by assuming particles can make elastic collisions only. The dynamics in the BUU model developed for heavy ion collisions at intermediate energies is therefore restricted to the baryonic level. Mesonic degrees of freedom enter via

 ©1991 The American Physical Society

nuclear potentials only. In the past, one has studied pion production by assuming that delta resonances have lifetimes longer than the nuclear reaction time; this is the so-called frozen delta approximation. The number of deltas at the end of the calculation then is equated to the total pion multiplicity.

Pion production cross sections and pion spectra have also been calculated in a perturbative manner in the subthreshold region by assuming energy-independent mean free paths for pions in baryonic matter [5,28]. We have, however, pointed out that a dynamical treatment of pions is needed in order to evaluate the relative importance of the collective mechanism and the individual nucleon-nucleon collision mechanism for subthreshold pion production [5].

Together with Wang and Randrup we have derived a coupled set of transport equations which governs the dynamical processes for a system of nucleons, deltas, and pions [29]. The aim of this work is to extend the framework for studying nuclear collisions from the baryonic level to hadronic level. This approach also enables us to treat dynamical pions in a BUU type of model in well-defined approximations.

In the present investigation we present numerical solutions of these coupled transport equations. We focus on the application of studying pion spectra, especially the mechanism for the concave shape of the pion spectra in relativistic heavy ion collisions and the systematics of this phenomenon.

The paper is organized as follows. We first present the model equations and a brief review of their derivation in the next section. In Sec. III we discuss the numerical realization procedure. We present results on the dynamics of pion production in relativistic heavy ion collisions in Sec. IV. In Sec. V we apply this model to study the mechanism for the concave shape of the pion spectra and confront our model calculations with the experimental data. Following that, we produce predictions of the dependence of the shape of the pion spectra on the beam energy, impact parameter, and mass of the projectile and target. We compare the shape parameter of the pion spectra with an approximate scaling function in Sec. VII. We conclude with a summary and discussion in the last section.

II. TRANSPORT EQUATIONS FOR HADRONIC MATTER

In Ref. [29] we start from an effective Lagrangian density including the free-baryon fields of nucleons and deltas, the meson fields of σ, ω, and π, as well as their interactions in the minimum coupling scheme. First, a set of coupled equations of motion for the density matrices of nucleons, deltas, and pions is derived. Subsequent Wigner transformations of these equations lead to a coupled set of transport equations for the phase-space distribution functions of nucleons, deltas, and pions. For the detailed derivation of these equations we refer the reader to Ref. [29]. The final result for the transport equation governing the time evolution of the baryon (nucleon and delta) phase-space distribution function $f_b(xp)$ is

$$\frac{\partial f_b(xp)}{\partial t}+\frac{\Pi^i}{E_b^*(p)}\nabla_i^x f_b(xp)-\frac{\Pi^\mu}{E_b^*(p)}\nabla_i^x U_\mu(x)\nabla_p^i f_b(xp)+\frac{M_b^*}{E_b^*(p)}\nabla_i^x U_s\nabla_p^i f_b(xp)=I_{bb}^b(xp)+I_{b\pi}^b(xp)\ , \quad (1)$$

where we have used the notation $x=(\mathbf{r},t)$. The collision terms $I_{bb}^b(xp)$ and $I_{b\pi}^b(xp)$ on the right-hand side of the equation are the rate of change of the baryon phase-space distribution function due to baryon-baryon collisions and baryon-pion collisions.

In the present investigation, we will not study the full equation with both scalar and vector mean-field potentials. Rather we wish to focus on the dynamics induced by the coupled collision terms for pions, deltas, and nucleons. For this purpose, we limit ourselves to the case of the presence of only a zeroth component of the vector mean-field potential to be able to compare with previous approaches.

With this assumption, the transport equation for the particular state b of the baryon (nucleon or delta) reads

$$\frac{\partial f_b(xp)}{\partial t}+\frac{\mathbf{p}}{E_b}\cdot\nabla_r f_b(xp)-\nabla_r U(x)\cdot\nabla_p f_b(xp)=I_{bb}^b(xp)+I_{b\pi}^b(xp)\ . \quad (2)$$

For (any charge state of) the pion we have

$$\frac{\partial f_\pi(xk)}{\partial t}+\frac{\mathbf{k}}{E_\pi}\cdot\nabla_r f_\pi(xk)=I_{b\pi}^\pi(xk)\ , \quad (3)$$

where $I_{b\pi}^\pi(xk)$ is the rate of change of the pion phase-space distribution function due to baryon-pion collisions. In the above equations we have used $p=(E,\mathbf{p})$ for the four-momentum of baryons and $k=(E_\pi,\mathbf{k})$ for that of pions.

It is noticed that the Vlasov term for the baryon transport equation is of the similar form as in the standard BUU equation, while for pions the Vlasov term contains only a drifting term due to the pion's velocity. In general, the pion field satisfies an inhomogeneous Klein-Gorden equation, but in deriving the transport equation for pions we have used the free-particle approximation for pions in order to simplify the manipulation within the density matrix formalism.

It has, however, been pointed out that the pion dispersion relation in the hot dense matter might be different from that in free space [30]. We therefore have to keep in mind that the potential energy for pions might be important and the present model calculation could allow us to study whether the present experimental pion production data at around 1 GeV/nucleon require any deviation from the free-space dispersion relation used in our calculations.

The collision terms are calculated by truncating the many-body correlations at the two-body level and using the G-matrix method to solve the equation of motion for the two-body correlation function [29–33]. The baryon-baryon collision term can be written as

$$I^b_{bb}(xp)=\pi\sum_{\alpha_1\alpha_2\alpha_3,m_s^b}\int\int\int\frac{M_bM_{\alpha_1}M_{\alpha_2}M_{\alpha_3}}{E_bE_{\alpha_1}E_{\alpha_2}E_{\alpha_3}}W^b_{bb}(p_1\alpha_1,p_2\alpha_2,p_3\alpha_3,p\alpha_b)$$
$$\times[f_{\alpha_2}(xp_2)f_{\alpha_3}(xp_3)\bar{f}_{\alpha_1}(xp_1)\bar{f}_b(xp)-\bar{f}_{\alpha_2}(xp_2)\bar{f}\alpha_3(xp_3)f_{\alpha_1}(xp_1)f_b(xp)]$$
$$\times\delta^{(4)}(p+p_1-p_2-p_3)\frac{1}{(2\pi)^9}d\mathbf{p}_1d\mathbf{p}_2d\mathbf{p}_3\ . \tag{4}$$

Here, the label $\alpha=(b,m_s,m_t)$, where $b=N$ or Δ, and m_s/m_t is the spin/isospin of the baryon. $W^b_{bb}(p_1\alpha_1,p_2\alpha_2,p_3\alpha_3,p\alpha_b)$ is the square of the transition matrix element in baryon-baryon collisions, which determines the transition rate. An explicit expression for W^b_{bb} can be given in terms of baryon-meson coupling constants [29]. Since we are not pursuing a first-principle theory at the present stage, the effect of the transition matrix element will be simulated by using the free-space cross sections as we will discuss in detail in the next section. In this respect, we take the same path as all other presently available relativistic dynamical models [7,26,27,34,39]. The above baryon-baryon collision term respects the Pauli exclusion principle as shown in the presence of $\bar{f}_\alpha(xp)=1-f_\alpha(xp)$ and $\bar{f}_b(xp)=1-f_b(xp)$. It is of the same structure as the NN collision term appearing in the standard BUU equation, but generalized to accommodate the four Δ states of the baryon.

The collision terms due to baryon-pion interactions can be written as

$$I^b_{b\pi}(xp)=\frac{\pi}{8}\sum_{\pi\alpha' m_s^b}\int\int\frac{M_bM_{\alpha'}}{E_b(p)E_{\alpha'}(p')}W^b_{b\pi}(\alpha'p',\pi k,\alpha p)\{[(1+f_\pi(xk))f_{\alpha'}(xp')\bar{f}_b(xp)$$
$$-f_\pi(xk)\bar{f}_{\alpha'}(xp')f_b(xp)]\delta^{(4)}(p'-k-p)$$
$$+[f_\pi(xk)f_{\alpha'}(xp')\bar{f}_b(xp)-(1+f_\pi(xk))\bar{f}_{\alpha'}(xp')f_b(xp)]$$
$$\times\delta^{(4)}(p'+k-p)\}\frac{1}{(2\pi)^6}d\mathbf{p}'d\mathbf{k} \tag{5}$$

and

$$I^\pi_{b\pi}(xk)=\frac{\pi}{16}\sum_{\alpha\alpha'}\int\int\frac{M_\alpha M_{\alpha'}}{E_\alpha(p)E_{\alpha'}(p')}W^\pi_{b\pi}(\alpha p,\alpha'p',\pi k)$$
$$\times[(1+f_\pi(xk))f_{\alpha'}(xp')\bar{f}_\alpha(xp)-f_\pi(xk)f_\alpha(xp)\bar{f}_{\alpha'}(xp')]\delta^{(4)}(p'-p-k)\frac{1}{(2\pi)^6}d\mathbf{p}d\mathbf{p}'\ . \tag{6}$$

In Eqs. (5) and (6) the index π has been used to specify the isospin quantum number of the pion. $W^b_{b\pi}(\alpha'p',\pi k,\alpha p)$ and $W^\pi_{b\pi}(\alpha p,\alpha'p',\pi k)$ are the square of the transition matrix element for the corresponding processes; again their effect will be simulated by using the free-space cross sections and the width of the resonances.

The above equations are the general expressions for the collision integrals; the matrix elements in these equations assure that only physical processes can happen. For example, only when b specifies a nucleon the first terms in Eq. (5) contribute, while only when b specifies a Δ the second terms contribute. It is worth noting that the fermion suppression factors and the boson enhancement factors are included in these collision terms and follow from the derivation.

Although the transport equations presented here are derived for a system of pions, nucleons, and delta resonances, they can be easily extended to contain higher resonances, such as the N^*. In the following we will treat N^*'s in a manner similar to that for delta resonances.

The advantage of the transport equations as presented above is that one can represent the phase-space distribution functions for nucleons, deltas, and pions by test particle distributions for the different species. With this, one is able to extend the powerful simulation techniques developed for the nonrelativistic case of the dynamical simulation of the phase-space distribution function of nucleons in heavy ion collisions to the relativistic coupled problem for nucleons, deltas, and pions. We discuss this procedure in detail in the next section.

III. NUMERICAL REALIZATION

The transport equations (2) and (3) for hadronic matter are highly coupled through the collision integrals. However, their solutions can be obtained numerically within the test particle method which was first introduced to nuclear physics by Wong [42]. The details of the application of the test particle method to solving the standard BUU equation can be found in Ref. [7].

In the test particle method one discretizes the continuous distribution function with a finite number of test particles representing individual phase-space cells. The test particles obey Newtonian equations of motion. The equations of motion for the baryon test particles corresponding to the solution of the transport equations (2) and (3) are

$$\frac{d\mathbf{r}}{dt}=\frac{\mathbf{p}}{E}\ , \tag{7}$$

$$\frac{d\mathbf{p}}{dt}=-\nabla_r U+\mathbf{D}^b_{bb}(p)+\mathbf{D}^b_{b\pi}(p)\ . \tag{8}$$

For the pion test particles, we obtain

$$\frac{d\mathbf{r}}{dt}=\frac{\mathbf{k}}{E_\pi}\ , \tag{9}$$

$$\frac{d\mathbf{k}}{dt}=\mathbf{D}^\pi_{b\pi}(k)\ . \tag{10}$$

Here $\mathbf{D}^b_{bb}(p)$, $\mathbf{D}^b_{b\pi}(p)$ are the changes of the baryon momentum distribution due to baryon-baryon collisions and baryon-pion collisions, respectively, in accordance with the collision integrals I^b_{bb} and $I^b_{b\pi}$. $\mathbf{D}^\pi_{b\pi}(k)$ is the corresponding change in the pion phase-space distribution due to baryon-pion collisions corresponding to the collision integral $I^\pi_{b\pi}$. They are calculated in the same manner as in the cascade models [38,39], namely, by discretizing the reaction time into small time steps and solving the collision integrals within each time step via a Monte Carlo simulation method.

In a first approximation we use a Skyrme-type density-dependent mean-field potential for the nucleons. It has been shown, however, that the stiff momentum-independent equation of state produces about the same amount of transverse momentum in heavy ion collisions as the available momentum-dependent parametrizations, and that the soft momentum-independent equation of state produces less [11]. For the observables studied by us, the use of all equations of state of the above forms yielded basically identical results. The mean-field potentials of the Δ and N^* are still very uncertain [35]. However, relativistic heavy ion collisions are expected to provide information about these potentials [36,37]. In this study we assumed that the potential energies of the Δ and N^* are the same as that of nucleons.

As in Ref. [7], we adopt the well-known Cugnon's parametrization for nucleon-nucleon elastic cross sections, for both the angular distribution and the total cross section. Following Ref. [43], Δ and N^* production cross sections for each charge state in all possible isospin channels have been estimated by using VerWest and Arndt's isospin decomposition formula [44] for pion production in nucleon-nucleon collisions.

Of the higher baryon resonances, only the $N^*(1440)$ is included. Resonances with even higher mass have negligible production cross sections in the energy range of interest here. The shape of the N^* resonance mass distribution is parametrized by a Breit-Wigner function with a constant width of 200 MeV [44].

The width for the Δ is parameterized following Kitazoe *et al.* [45] as

$$\Gamma(q)=\frac{0.47q^3}{[1+0.6(q/m_\pi)^2]m_\pi^2}\ , \tag{11}$$

where q is the momentum of the pion.

During each time step, the decay probability of the Δ's and N^*'s present in the system is determined by an exponential law using the proper time obtained from their widths. The branching ratios for the allowed final states are determined from the appropriate Clebsch-Gordan coefficients. The cross section for the pion-nucleon resonance is also parametrized using the Breit-Wigner formula with the maximum cross section from the experimental data [46],

$$\sigma_{\max}(\pi^+p\to\Delta^{++})=\sigma_{\max}(\pi^-n\to\Delta^-)=200\text{ mb}\ , \tag{12}$$

$$\sigma_{\max}(\pi^0p\to\Delta^+)=\sigma_{\max}(\pi^0n\to\Delta^0)=135\text{ mb}\ , \tag{13}$$

$$\sigma_{\max}(\pi^-p\to\Delta^0)=\sigma_{\max}(\pi^+n\to\Delta^+)=70\text{ mb}\ , \tag{14}$$

$$\sigma_{\max}(\pi^-p\to N^{*0})=\sigma_{\max}(\pi^0n\to N^{*0})=50\text{ mb}\ , \tag{15}$$

$$\sigma_{\max}(\pi^+n\to N^{*+})=\sigma_{\max}(\pi^0p\to N^{*+})=50\text{ mb}\ . \tag{16}$$

The phase-space occupation factors for the final state of the fermions, $1-f_b(xp)$ in Eqs. (5) and (6), are treated via a Monte Carlo rejection method. Since the computation of all possible final-state phase-space occupation factors is a very time-intensive task, we have developed a technique to store the six-dimensional phase-space occupation probability at every time step on a lattice [47]. In this way we are able to use a large number of test particles (>100) to represent a real particle in the reaction of two heavy nuclei while using a reasonable amount of CPU time. BUU type of calculations for heavy system have been hindered using the old way of evaluating Pauli blocking factors. For reactions involving intermediate mass nuclei, as many as 400 test particles per real particle have been used. For the implementation of this technique, we have to, however, make use of the locality in time and the mass-shell condition for the energy.

The final-state phase-space occupation probability factors for bosons, $1+f_\pi(xp)$, cannot be treated by conventional rejection methods, because the possible range of values of this function is not between 0 and 1. However, it is possible to introduce a cutoff F such $F>\max[1+f_\pi(xp)]$ for all coordinate values (x,p) during the course of the nuclear collision. By multiplying the interaction matrix element by F and dividing $[1+f_\pi(xp)]/F$ one can use the conventional rejection technique on this scaled occupation probability factor.

In the present calculation the mean boson phase-space occupation probabilities are on the order of $\langle f_\pi\rangle\approx 5\times10^{-2}$, because we have, for example, ≈ 50 pions of three different isospin substates distributed over a total phase-space volume of $\approx 400h^3$ for central La+La collisions at 1.35 GeV/nucleon beam energy. Thus the effect of stimulated emission of pions due to the effect of the boson enhancement factor is negligible in the case studied here. In nucleus-nucleus collisions at CERN energies, however, this may not be the case. Depending on the assumptions for pion freeze-out and expansion of the hadronic system, pion phase-space occupation probabilities may become comparable to 1, and one may introduce a nonzero chemical potential for pions. Kataya and Ruuskanen [23] have shown that then one can also obtain a concave p_t spectrum for negative pions due to this effect.

IV. DYNAMICS OF PION PRODUCTION

To gain some insight into the dynamical properties of relativistic heavy ion collisions and to get some familiarity with the dynamical characteristics of our model, we show in Fig. 1 the time evolution of the accumulated total baryon-baryon collision numbers and the reaction rates for several relevant collision processes. In the model explicit isospin degrees of freedom have been used; the quantities shown in the figure are the sums over all possible isospin channels.

The particular choice of the system Ca+Ca at a beam energy of $E/A=1.8$ GeV and impact parameter $b=0$ is made in order to compare with Cugnon's cascade calculation [39]. The overall time dependence of the total collision number and reaction rates is similar to that of the cascade calculation. The accumulated baryon-baryon collision number saturates at around 10–15 fm/c. After this time, mainly Δ decays and pion reabsorptions are present. We see that the Δ destruction processes, $N\Delta\rightarrow NN$ and $\Delta\rightarrow N\pi$, set in slightly later than the $NN\rightarrow N\Delta$ process, because the former processes need an appreciable accumulation of Δ's, and because the Δ has a finite lifetime. The Δ decay rate is always higher than that of the formation of this resonance.

It is of interest to note the quantitative differences between our model calculations and the cascade model calculations. The saturated number of total baryon-baryon collisions calculated in the present model is about 15% smaller than that of the cascade model. This is mainly due to the better treatment of the Pauli blocking factor and the inclusion of the mean field in our model. The time-integrated cross section for the Δ reabsorption process ($N\Delta\rightarrow NN$) in the present model is about twice of that in the cascade model. Consequently, the total number of pions observed in the final state is about 30% less than that in the cascade model. A later modified cascade calculation [40] shows that the discrepancies between the experimental data and the cascade calculation on pion production in proton, pion, and heavy ion induced reactions can be removed if one artificially multiplies the cross section $\sigma(N\Delta\rightarrow NN)$ by a factor of 3 without changing the cross section $\sigma(NN\rightarrow N\Delta)$. This has been explained as an indication of the enhancement of the pion reabsorption in nuclear medium and the underestimation of the pion reabsorption in their model. However, in our calculation the medium effect explanation is not necessary, and the total pion production cross sections are in agreement with data (see below).

Since we are interested in the properties of pions, it is crucial to know the time evolution of the source of the pions. In Fig. 2 the population of free pions and pions still bound inside excited baryons (unborn pions) is displayed for the system La+La at a beam energy of 1350 MeV per nucleon and $b=1$ fm. It is seen that the total number of pions, Δ's, and N^*'s freezes out at around $t=20$ fm/c at a value which is in good agreement with experimental data [6]. The overall time dependence of our bound and unbound pion multiplicities is similar to the one obtained from the cascade calculation.

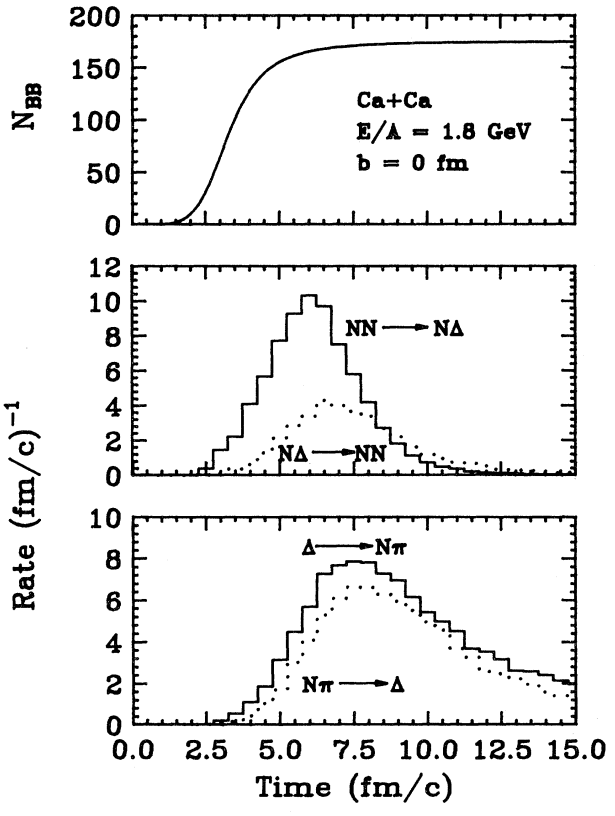

FIG. 1. Upper figure: Accumulation of the total number of baryon-baryon collisions in the reaction of Ca+Ca at $E/A=1.8$ GeV and impact parameter $b=0$ fm. Lower figure: Time evolution of the reaction rate for the specified processes in the same reaction.

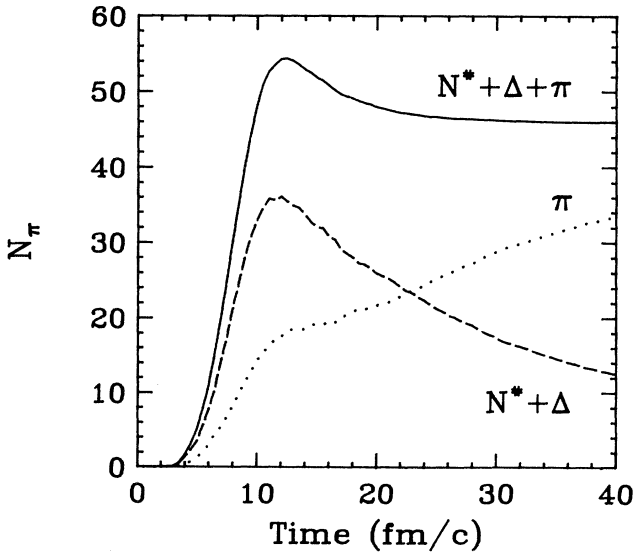

FIG. 2. Time evolution of the population of free pions, Δ's and N^*'s in central collisions of La+La at $E/A=1350$ MeV.

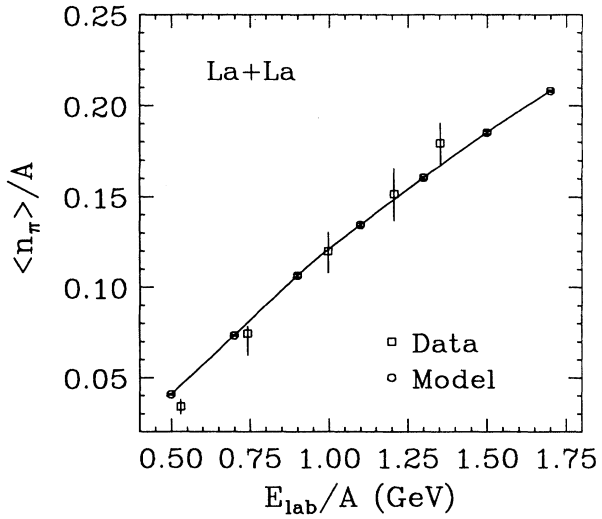

FIG. 3. Excitation function of the pion multiplicity in central collisions of La+La. The squares are the experimental data of Ref. [6], and the round plot symbols on the solid line are the model calculations.

In Fig. 3 we compare the excitation function of the pion multiplicity with that of the experimental data for central collisions of La+La. The round plot symbols on the solid line are our calculated results, and the square symbols with error bars are the experimental data [6]. A good agreement can be seen in the whole energy range. Similarly good results have been obtained with a VUU model [41]. In Ref. [41] a comparison of the data to existing cascade model calculations is shown as well, and a clear overprediction is observed for this model.

V. MECHANISMS FOR THE CONCAVE SHAPE OF PION SPECTRA

In this section, we apply our model to study the mechanism that causes the concave shape of pion spectra in central heavy ion collisions at around 1 GeV/nucleon. Several hypotheses have been made by the groups who discovered this effect in order to explain their experimental results. These include the superposition of thermal pions and the pions from the final-state Δ decays, higher resonances [13] and the effect of baryon flow on the pions [16]. Based on a simplified hydrodynamical model calculation [17], it was also conjectured that the concave shape of the pion spectra may come from an isotropic hydrodynamical expansion of the hot compressed nuclear matter.

The cascade model predicts purely thermal pion spectra [13], although it has been very successful in predicting many other experimental observables in relativistic heavy ion collisions. The original BUU model uses the frozen delta approximation and qualitatively reproduces the two-temperature pion spectra [16]. The origin of this agreement, however, was not investigated.

In a previous publication [18] we proposed that the concave shape of the pion spectra might come from different contributions of Δ resonances produced early and late during the course of the heavy ion collision. Here we explore this idea in more detail and compare our model calculations with the available experimental data.

A. Model calculation for the pion spectrum

In Fig. 4 we show the number of pions per energy interval for the La+La reaction, $(1/PE)(dN/dE)$, as a function of the pion kinetic energy, where P is the momentum and E is the total energy of the pions.

The time chosen for the figure, $t=20$ fm/c, approximately the freeze-out time; by this time most of the baryon-baryon collisions have ceased, but a large fraction of the excited baryons produced have not decayed yet.

The real pions which are not bound in resonances are represented by the solid histogram. For a thermally equilibrated dilute pion gas at a temperature T, we can use the Boltzmann distribution function

$$\frac{1}{PE}\frac{dN}{dE}=c\exp\left[-\frac{E_{\rm kin}}{T}\right]. \tag{17}$$

As we can observe from Fig. 4, the free pions at freeze-out can be well described with a Boltzmann distribution of temperature 78 MeV (straight-line fit).

By assuming a sudden decay of all Δ's and N^*'s at freeze-out, the contribution to the pion spectrum from bound pions can be obtained. These are shown by the dashed histogram. It is clear that these pions do not show the same temperature as the pions which are already free at freeze-out time, but indicate a lower temperature.

If we superimpose the two contributions to the pion

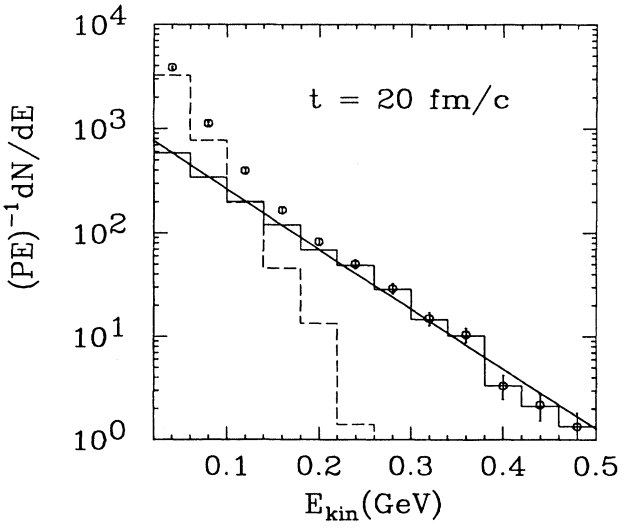

FIG. 4. Calculated contributions to the pion spectrum from pion already free (solid histogram) and still bound in baryonic resonances (dashed histogram) as well as their sum (circles) at $t=20$ fm/c.

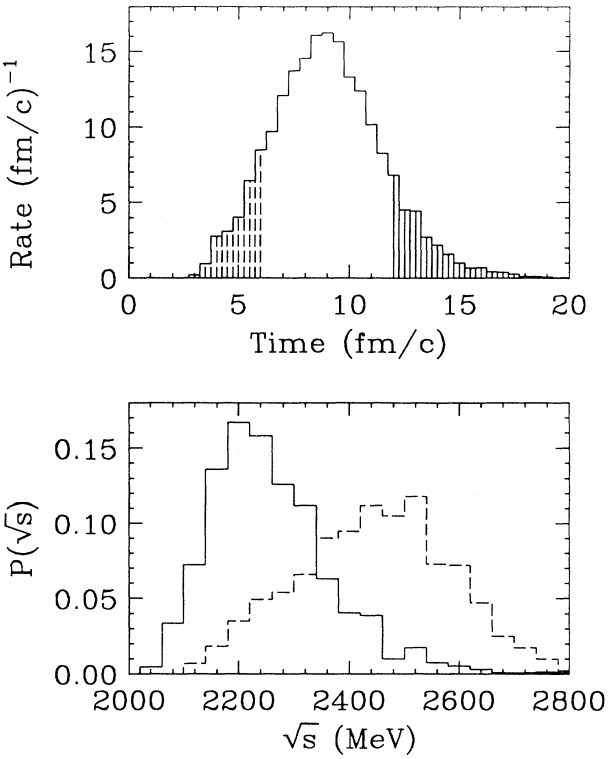

FIG. 5. Upper part: Rate of nucleon-nucleon collisions which lead to the formation of a Δ during the central La+La reaction at $E/A=1350$ MeV. Lower part: Probability distribution for the total energy in the nucleon-nucleon center-of-mass system. The dashed histogram corresponds to the early collisions ($t \leq 6$ fm/c, dashed hatched area in the upper part), and the solid histogram represents the late nucleon-nucleon collisions ($t \geq 12$ fm/c, solid hatched area in the upper part).

spectrum, we obtain the result which is represented by the round plot symbols. The error bars are of statistical nature since we solve the transport equations [Eqs. (2) and (3)] with a Monte Carlo integration procedure. The concave shape obtained in this way clearly hints at a pion spectrum with a two-temperature appearance. The low temperature is about 50 MeV for pions with $E_{\rm kin} \leq 0.2$ GeV and the higher one is about 78 MeV for pions with $E_{\rm kin} \geq 0.2$ GeV.

We note that the total pion spectrum obtained at $t=20$ fm/c (Fig. 4) is almost the same as that obtained at $t=40$ fm/c when we stop our calculation. The reason for this is that between these two time instances the Δ's and N^*'s are almost moving freely during this expansion phase before they decay.

B. Concave pion spectra

What is the reason for the pions that are still bound at freeze-out to show a lower temperature? We attempt to answer this question in Fig. 5. The upper part of Fig. 5 shows the rate of processes

$$N+N \rightarrow N+\Delta \qquad (18)$$

during the La+La reaction. The lower part of the figure displays the probability distribution of baryon-baryon center of mass energies, $\sqrt{s}$, for two different time intervals during the course of the heavy ion reaction, as extracted from the computer calculation. The dashed histogram corresponds to all baryon-baryon collisions of the type Eq. (18) during the initial compressional phase of the reaction (dashed hatched area in the upper part of the figure), $t \leq 6$ fm/c. The solid histogram corresponds in the same way to all collisions for $t \geq 12$ fm/c (solid hatched area).

We can clearly see that the early baryon-baryon collisions are on average more energetic than the later ones. This is because the central rapidity region is initially free of baryons, but is increasingly more populated as the reaction proceeds. A subsequent interaction of a nucleon at central rapidity with a nucleon at target or projectile rapidity thus becomes more and more probable towards the later time in the reaction. Since it is less energetic than a reaction of a nucleon at projectile rapidity and one at target rapidity (the only kind possible in the initial stage of the reaction), the Δ's produced later are less energetic than the ones produced earlier, and the different contributions to the kinetic energy spectrum of the pions can be understood.

The pion spectra shown in Fig. 4 are the results of the full dynamical evolution of the system, and this also includes the reabsorption of pionic excitations. We therefore have to ask what the effect of pion reabsorption and rescattering on the pion spectrum is.

In the present model pions can be reabsorbed through the two-step mechanism, namely, $N\pi \rightarrow \Delta(N^*)$ and $N\Delta(N^*) \rightarrow NN$.

To illustrate the effect of pion reabsorption and rescattering on the pion spectrum, we compare in Fig. 6 the primordial π^- spectrum with the final one obtained at $t=40$ fm/c from the full dynamical evolution for the

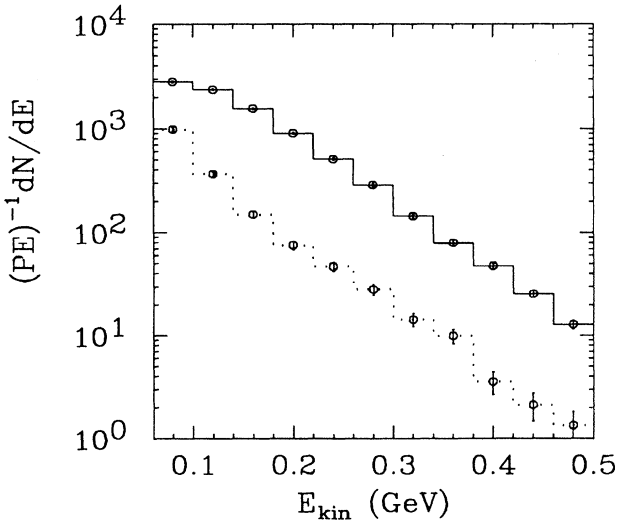

FIG. 6. Comparison between the spectra of primordial pions (solid histogram) and final pions (dotted histogram).

La+La reaction. The primordial pions are obtained by recording the momentum, mass, and isospin of all Δ's and N^*'s when they are first produced during the course of the reaction, and by calculating the pion spectrum which would be obtained if all of these baryonic resonances were to decay right after they are formed, and the resulting pions would propagate without further interaction from then on. The primordial pions are represented by the round plot symbols on the solid histogram, and the final pions are represented by the plot symbols on the dotted histogram.

We first notice the large difference in the normalizations of the two histograms: The number of finally escaping pions is only on the order of 10% to 20% of the total number of pionic excitations generated during the course of the heavy ion reaction.

Second, we see that the primordial pion spectrum does not show the concave shape observed in the final distribution. Due to the effect described above, the primordial pion spectrum is, however, not quite of the Boltzmann type as predicted by the thermal equilibrium model calculations [17,48,49]. The reason for this additional shape change lies in the energy dependence of the elementary pion absorption cross sections obtained from detailed balance. High-energy pions with kinetic energy larger than 0.2 GeV are rescattered or reabsorbed at a higher rate than low-energy ones.

In addition, pion absorption is a two-step process and thus dependent on the square of the nucleon density. This also favors the reabsorption of the higher-energy pions produced early in the reaction (when the baryon density was high) over the reabsorption of lower-energy pions produced later in the heavy ion reaction (when the baryon density was lower). Clearly, a dynamical calculation of pion reabsorption is thus essential for the correct explanation of pion energy spectra, and a calculation utilizing an energy-independent pion mean free path in nuclear matter is insufficient.

From the above arguments based on Figs. 5 and 6, it is clear that we do not have only two contributions of different temperature to the pion spectrum, but rather a continuous change from the initial high-temperature contribution to the final low temperature. The formation of the concave shape of the pion spectra is due to the gradual change of mean energies of the formed baryon resonances and the gradual change of reabsorption conditions during the course of the reaction.

In the study of pion spectra in relativistic heavy ion collisions an important question is to what extent the slope of pion spectra reflects the true temperature of the system in the early high-compression phase of the reaction. From the comparison of the two spectra shown in Figs. 4 and 6, we see that the higher temperature extracted from the pion spectra in the final state more accurately reflects the temperature of the system in its early phase. However, one should use caution in applying the term "temperature," because what we observe is not the consequence of an equilibrated system, but rather of a nonequilibrium transport process of a system on its path towards kinetic equilibration.

Within the present transport model, one can also test the other hypotheses made to explain the concave shape of the pion spectra. By studying the dependence of the shape of the pion spectra on the nuclear equation of state [18], it is found that one should at most expect a small effect on the pion spectra from the baryon collective flow.

The effect of higher resonances on the pion spectrum, such as that of $N^*(1440)$'s included in the present model, has been studied by turning off the reaction channels involving N^*'s. It is found that the presence of N^*'s has only a very small effect due to their small production cross sections in the energy range interested here. This finding is in agreement with that of Randrup from the study of the hadronic matter equilibration process [38]. It was found that as long as the beam energy remains of the order of 1 GeV/nucleon it suffices to include only the Δ resonance. However, at higher energies, $E_{\text{beam}} \geq 2$ GeV/nucleon, higher baryon resonances as well as direct multiple pion production grow increasingly important in the reaction process, and their effects on the pion spectra remain to be explored.

C. Comparison with experimental data

In Fig. 7 we compare our model calculation with experimental data for central ($b < 2.8$ fm) reactions of La+La at a beam energy of 1350 MeV per nucleon. The experimental π^- number distribution, $(PE)^{-1}dN/dE$ at 90°±30° in the center of mass of the target and projectile, is shown as a function of pion kinetic energy and represented by the round plot symbols. The data can be well fitted by a two-temperature fit with a χ^2 per degree of freedom of 0.9, whereas the minimum χ^2 per degree of freedom is 3.4 for a one-temperature fit [15]. For comparison, the one-temperature fit ($T=49$ MeV) to the data is shown with the dashed line. Our calculations are represented by the histogram. Calculation and data both

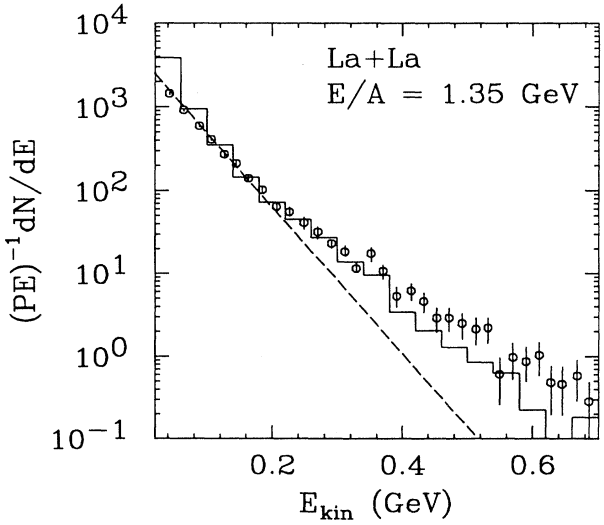

FIG. 7. Comparison between calculations (histogram) and the experimental data of Ref. [15] (plot symbols). The dashed line is the one-temperature fit to the experimental data with temperature $T=49$ MeV.

show a clear deviation from the one-temperature fit. The data are in reasonable agreement with our calculation.

A slight tendency of underpredicting the higher-energy pions of energy $E_{\rm kin} \geq 0.4$ GeV is noticed. One of the reasons is that a semiclassical momentum distribution has been used to initialize the nucleons; therefore, the calculation lacks the quantum high-momentum components. This is a problem we share with all the other semiclassical dynamical models. In the lowest-energy bin, we overpredict the data by a factor of 2–3, which is primarily due to the fact that we neglect the Coulomb interaction of the pions with the nuclear system.

In Fig. 8 we perform another comparison between our calculation and the experimental data for central collisions of Ar+KCl at a beam energy of $E/A = 1.8$ GeV. This is the experimental data set in which the two-temperature structure of the pion spectrum was first found [13]. Again, the experimental data are displayed by the round plot symbols, and the solid histogram is our calculation. The dashed curve is a one-temperature fit to the spectrum with $T = 63$ MeV.

As can be seen from the figure, the pion energy spectrum shows a deviation from the simple exponential law for pion energies greater than 0.5 GeV. A fit with two slope parameters ($T_1 = 58$ MeV and $T_2 = 110$ MeV) reproduces the whole spectrum. Similar to the situation in La+La reactions shown in Fig. 7, experimental data and model calculation agree quite well.

It is well known that the cascade models with Δ resonances and their decays predict a single exponential spectrum. In principle, the main differences between our hadronic transport model and the cascade models are the inclusion of the mean field for baryons and a more proper treatment of the Pauli blocking in the present model.

The agreement between our model calculations and the available experimental data indicates that to correctly describe the experimental observables in heavy ion collisions of 1–2 GeV/nucleon beam energies, it is necessary to include the mesonic degrees of freedom explicitly, while still keeping the baryon mean field. This is because in this energy domain the long-range nucleon-nucleon interactions are still sufficiently significant that the particles are not free but moving in a varying mean field in both space and time.

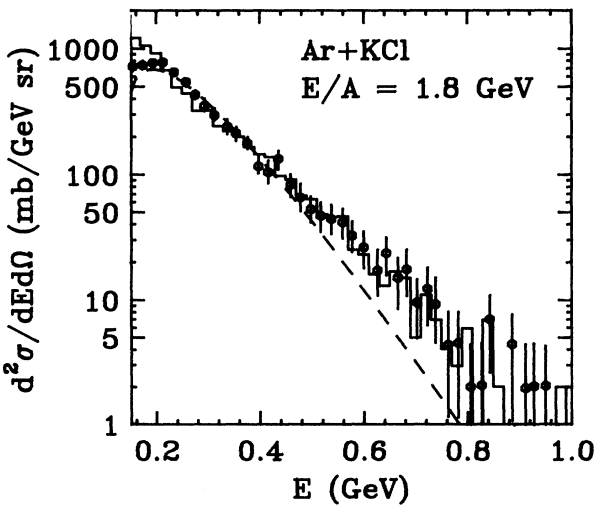

FIG. 8. Comparison between calculations (histogram) and the experimental data of Ref. [13] (plot symbols). The dashed line is the one-temperature fit to the experimental data with temperature $T = 63$ MeV.

VI. SYSTEMATICS OF PION SPECTRA

From our previous discussions, we see that what is important for reproducing the experimentally observed concave shape of the pion spectra is the correct description of the effects of the reaction dynamics on pion production and absorption. Pions in the high-temperature component are mainly produced in the early high-compression phase of the reaction, probably during the first one or two nucleon-nucleon collisions per nucleon. On the other hand, low-energy pions are mainly produced in the late expansion phase of the reaction. Pion spectra carry indeed interesting information about the space-time dynamics of heavy ion collisions. More of this information can be obtained by studying the dependence of the shape of the pion spectra on the beam energy, mass, and impact parameter.

The systematic experimental study of the concave shape of the pion spectra is underway on SIS/Gesellschaft für Schwerionenforschung by the KAOS Collaboration [50], it is therefore interesting to study these systematics based on our model calculations also. Moreover, a comparison between the two systematic studies will further determine the mechanism that causes the concave shape of the pion spectra and further test our model ingredients.

A. Energy dependence

We first study the energy dependence of the shape of the pion spectra in central collisions of La+La. In experiments one usually measures the pion spectrum at around 90° in the c.m. system in order to avoid the "corona effect" [13], so that reliable information about the dynamics and properties of the hot and dense matter in the participant region can be extracted. All the spectra presented in the following are then calculated in the c.m. system at 90°±30° in accordance with the experimental situation of the KAOS Collaboration [50].

Pion spectra in central collisions have been calculated for beam energies from 0.5 GeV/nucleon to 2.1 GeV/nucleon; typical ones are displayed in the upper part of Fig. 9. Pion spectra at beam energies below 0.7 GeV/nucleon can be well described by a one-temperature Boltzmann distribution. This is because in this energy range the nucleon-nucleon inelastic cross section is small; only the first collision of a nucleon with target rapidity and a nucleon with projectile rapidity can effectively produce pions. For beam energies greater than 0.7 GeV/nucleon, if one fits the lower-energy part of the spectrum with a single exponential distribution it is seen

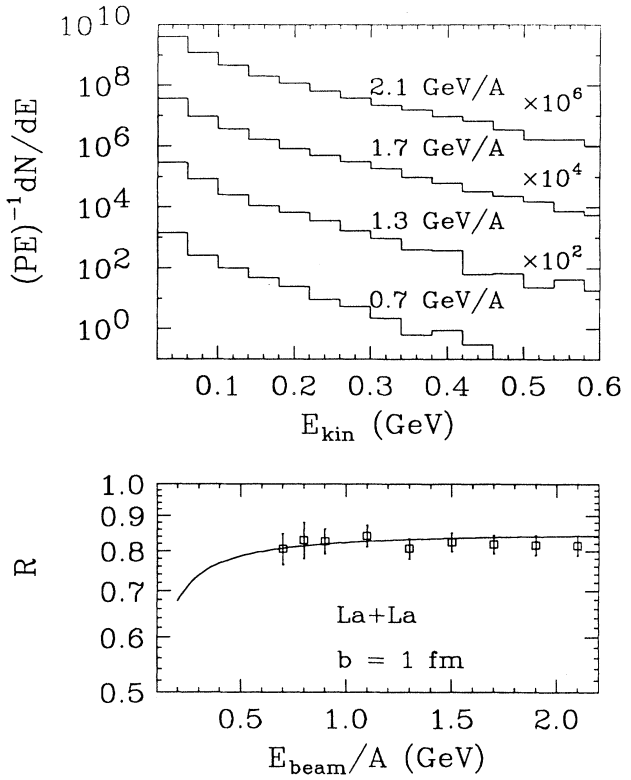

FIG. 9. Upper figure: Calculated energy dependence of the pion spectra at 90°±30° in the center-of-mass frame for La+La reactions at impact parameter $b=1$ fm. Lower figure: Energy dependence of the shape parameter R of the pion spectra shown in the upper figure. The solid line represents the analytic scaling function of Eq. (21).

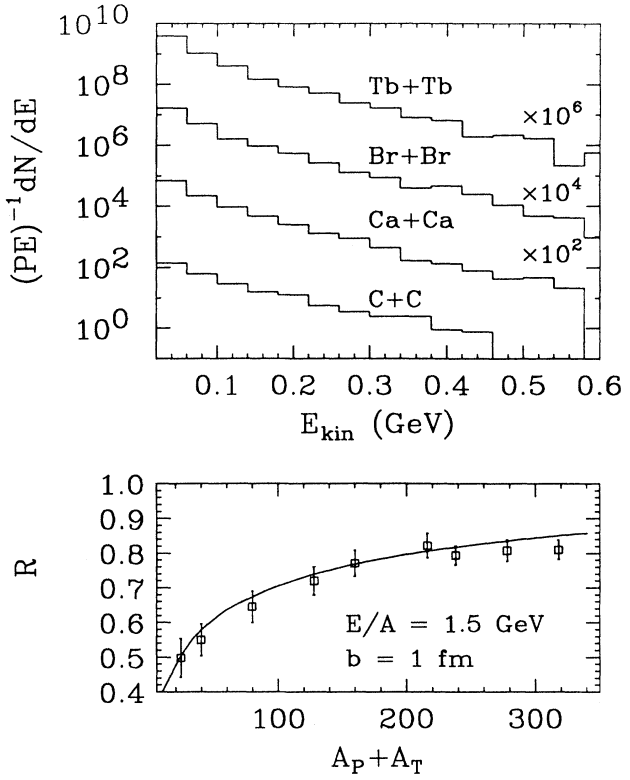

FIG. 10. Upper figure: Calculated mass dependence of the pion spectra at 90°±30° in the center-of-mass frame for a beam energy of 1.5 GeV/nucleon and impact parameter $b=1$ fm. Lower figure: Mass dependence of the shape parameter R of the pion spectra shown in the upper figure. The solid line represents the analytic scaling function of Eq. (21).

that the deviation of the spectrum from the single exponential distribution increases as the beam energy increases up to around 1.5 GeV/nucleon. The general feature observed here is in agreement with the experimental findings [15]. However, the tendency is not so obvious at beam energies above 1.5 GeV/nucleon.

As can be seen, the slope of high-energy pions also increases as the beam energy increases. As we have discussed in the last section, pions in this high-"temperature" component are produced in the early high-compression phase of the reaction. The slope of the high-energy pions reflects the amount of energy deposited in the participant region via baryon excitations, which is monotonically increasing with beam energy.

B. Mass dependence

In Fig. 10 the upper part shows our predictions on the mass dependence of the pion spectrum. All calculations are performed for symmetric systems at a beam energy of 1.5 GeV/nucleon and an impact parameter of 1 fm.

For light systems, such as C+C and Ne+Ne (not shown), the spectra can be well described by a one-temperature Boltzmann distribution. The reason for that is the following, for light systems the size of the participant region is small which is compatible with the mean free path of the nucleon, therefore on average particles only suffer one collision during the course of the reaction. For heavier systems from Ca+Ca to Tb+Tb, the situation is different. If one fits the lower-energy part of the spectrum with a single exponential distribution, one sees that the deviation of the spectrum from the single exponential distribution increases as the mass of the system increases. This feature of the mass dependence also agrees with the experimental results. Looking at the experimental pion spectra shown in Figs. 7 and 8, the deviation of the spectrum from the single exponential law in La+La is much larger than that in Ar+KCl, given the fact that the beam energy per nucleon in the La+La reaction is 450 MeV smaller than in the reaction of Ar+KCl. We also observed that the slope of high-energy pions is almost independent of the mass of the colliding nuclei.

C. Impact parameter dependence

Little knowledge of the impact parameter dependence of the pion spectra is presently available from experimen-

tal data. The KAOS Collaboration has thus planned to study this dependence. In particular, a change in the slope of high-energy pions with centrality might indicate a thermal origin for these pions, while a similar slope would favor a dynamical decay process.

Our predictions on the impact parameter dependence of the pion spectrum are shown in the upper part of Fig. 11. The reaction of Ar+KCl at a beam energy of 1.8 GeV/nucleon has been chosen. It can be seen that the spectra are almost parallel to each other and show a concave shape for impact parameters smaller than 3 fm. For impact parameters larger than 5 fm the spectra show only one temperature component. This is because at large impact parameters too few particles are inside the collision zone, and pions are produced in first collisions only.

In experiments the centrality of the reaction is usually measured in terms of the charged particle multiplicity, in this case charged pions. In our model calculations there is a one-to-one correspondence between the impact parameter and the multiplicity of charged pions in the final state. It will therefore be possible to make a direct comparison between our calculations and the coming experimental data from the KAOS Collaboration.

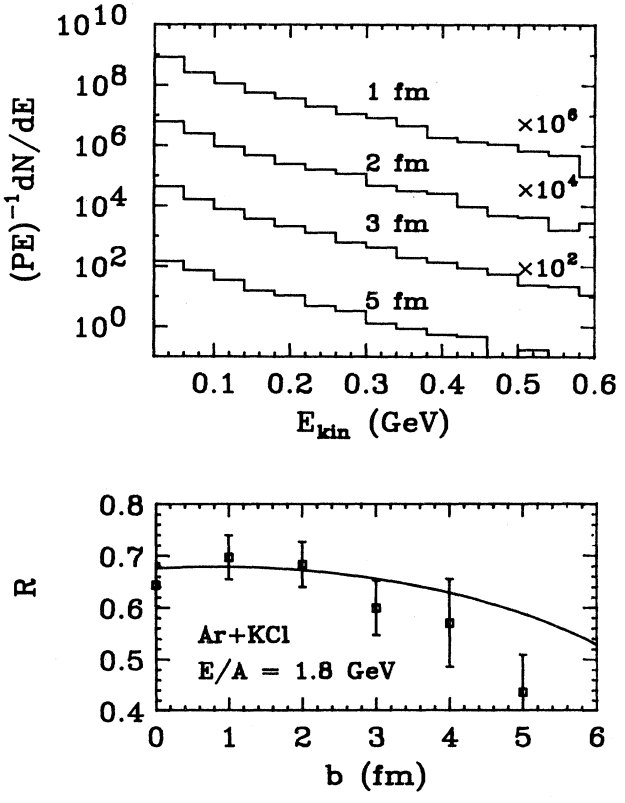

FIG. 11. Upper figure: Calculated impact parameter dependence of the pion spectra at 90°±30° in the center-of-mass frame for Ar+KCl reactions at beam energy of 1.8 GeV/nucleon. Lower figure: Impact-parameter dependence of the shape parameter R of the pion spectra shown in the upper figure. The solid line represents the analytic scaling function of Eq. (21).

VII. APPROXIMATE ANALYTIC SCALING FUNCTION

To describe the shape of the pion spectrum quantitatively and further study its dependence on beam energy, mass, and impact parameter, we perform a least-squares fit to the spectrum with a two-temperature distribution function

$$(PE)^{-1}dN/dE = A_1 \exp(-E_{\rm kin}/T_1) + A_2 \exp(-E_{\rm kin}/T_2) , \tag{19}$$

and define the shape parameter as

$$R = \frac{A_1 T_1}{A_1 T_1 + A_2 T_2} . \tag{20}$$

With T_1 we refer to the lower temperature in the two-temperature fit. It should be noted that this temperature is not the same as obtained by fitting the lower-energy part of the spectrum with a single exponential function. R represents the fraction of the area in the first exponential. It is approximately equal to the fraction of the pion yield in the first exponential [15].

The shape parameters as extracted from our computer calculations are plotted in Figs. 9, 10, and 11 as functions of beam energy, mass, and impact parameter, respectively. The energy dependence of the shape parameter is rather flat. As a function of the total mass of the system, R increases from about 0.5 to 0.8 when the total masses of the system grows from 24 to 160. For heavier systems, R saturates at around 0.8. For Ar+KCl collisions at a beam energy of 1.8 GeV/nucleon, the shape parameter is about 0.7 for impact parameters smaller than 2 fm, it then decreases to about 0.4 at $b=5$ fm.

In order to understand the scaling behavior of the shape parameter R we may attempt to formulate approximate scaling laws, based on our knowledge of the mechanism that causes the concave shape of the pion spectra. As we have discussed previously, pions in the higher-temperature component are mainly produced in the early high-compression phase during the course of the reaction. To obtain an approximate scaling function we assume that pions in the higher-temperature component are completely coming from first collisions in the early phase of the reaction. This approximation is valid for beam energies which are not too high. To contribute to the lower-energy component, at least one of the colliding nucleons has to have had at least one previous collision to transport it into the "midrapidity source." We use Poisson statistics for the probability distribution of the number of nucleon-nucleon collisions. Under these simplifying assumptions, the scaling function for the shape parameter is given by

$$R = \frac{1-e^{-\bar{n}}-\bar{n}e^{-\bar{n}}}{1-e^{-\bar{n}}} , \tag{21}$$

where $\bar{n}$ is the average number of nucleon-nucleon collisions per nucleon [51],

$$\bar{n}=\frac{\lambda_p\lambda_d\sigma_{nn}(E)\int_{\mathcal{O}}dxdy\int_{-\infty}^{\infty}dz_1dz_2\rho_t(x^2+y^2+z_1^2)^{1/2}\rho_p(x^2+y^2+z_2^2)^{1/2}}{\frac{1}{2}\int_{\mathcal{O}}dxdy\int_{-\infty}^{\infty}dz[\rho_p(x^2+y^2+z^2)^{1/2}+\rho_t(x^2+y^2+z^2)^{1/2}]} . \tag{22}$$

Here $\sigma_{nn}(E)$ is the energy-dependent total nucleon-nucleon cross section. The integrations over x and y are performed over the geometrical overlap area $\mathcal{O}$ with the Monte Carlo integration method. λ_p is a correction factor resulting from the fact that the final-state phase space for the scattering nucleons is partially Pauli forbidden. With use of geometrical considerations, it can be approximated by

$$\lambda_p=\left[1-\frac{2p_F^3-\frac{1}{2}h^2(3p_F-h)}{(p_F+p_b)^3}\right]^2 , \tag{23}$$

with $h=(p_F-p_b)\theta(p_F-p_b)$. λ_d is another correction factor used to include properly the effect of energy degradation and pion reabsorption. A constant of 0.6 has been used in our calculations.

Even though we expect the above scaling function for the shape parameter to be only an approximation, we can still compare it with the numerical values extracted from the calculated spectra. The results obtained from Eq. (21) are displayed by the solid lines in the lower parts in Figs. 9, 10, and 11. As can be seen the qualitative features of the numerical calculations are reproduced, and the gross features of the shape parameter and therefore the systematics of pion spectra in relativistic heavy ion collisions at beam energies around 1 GeV/nucleon can be understood in terms of the simple scaling arguments presented here.

VIII. SUMMARY

We have presented a hadronic transport model for studying relativistic heavy ion collisions. This model is based on solutions of a set of coupled transport equations for the phase-space distribution functions of nucleons, baryon resonances, and pions. The model can be seen as an extension of the BUU model from the baryon dynamics level to the hadron dynamics level.

An application of the model to the study of the pion spectrum shows that the shape of the pion spectrum reflects the effect of the reaction dynamics on pions; the mechanism for the concave shape of the pion spectra in central heavy ion collisions is found to be due to the different contributions of the delta resonances produced early and late during the course of the reaction. The available experimental pion spectra have been reproduced. The systematic study of the shape of the pion spectra indicates that the concavity of the pion spectra increases with both the beam energy and the mass of the colliding nuclei, and decrease with impact parameter.

An approximate scaling function for the shape parameter of the pion spectra has been derived from a Glauber-type multiple collision model to understand the systematics of the pion spectra. Upcoming experimental results from the KAOS Collaboration on the systematics of the concave shape of the pion spectra are expected to further test our model predictions.

We conclude from our study that in heavy ion collisions of beam energies around 1 GeV/nucleon it is necessary to treat mesonic degrees of freedom explicitly, without neglecting the nuclear mean field. This is important to understand the observables sensitive to the dynamical degrees of freedom in relativistic heavy ion collisions and to reliably infer properties of hot and dense matter produced in these collisions.

ACKNOWLEDGMENTS

We acknowledge helpful discussions with G. F. Bertsch, P. Danielewicz, V. Koch, J. Randrup, E. V. Shuryak, and S. J. Wang. This research was supported by the National Science Foundation under Grant PHY-8906116.

[1] R. Stock, R. Bock, R. Brockmann, J. W. Harris, A. Sandoval, H. Ströbele, K. L. Wolf, H. G. Pugh, L. S. Schroeder, M. Maier, R. E. Renfordt, A. Dacal, and M. E. Ortiz, Phys. Rev. Lett. **49**, 1236 (1982).

[2] H. Stöcker and W. Greiner, Phys. Rev. **137**, 277 (1986).

[3] C. Gale and J. Kapusta, Phys. Rev. C **35**, 2107 (1987).

[4] W. Bauer, G. F. Bertsch, W. Cassing, and U. Mosel, Phys. Rev. C **34**, 2127 (1986).

[5] W. Bauer, Phys. Rev. C **40**, 715 (1989).

[6] J. W. Harris, R. Bock, R. Brockmann, A. Sandoval, R. Stock, H. Ströbele, G. Odyniec, H. G. Pugh, L. S. Schroeder, R. E. Renfordt, D. Schall, D. Bangert, W. Rauch, and K. L. Wolf, Phys. Lett. **153B**, 377 (1985); Phys. Rev. Lett. **58**, 463 (1987).

[7] G. F. Bertsch and S. Das Gupta, Phys. Rep. **160**, 189 (1988).

[8] G. F. Bertsch, H. Kruse, and S. Das Gupta, Phys. Rev. C **29**, 673 (1984).

[9] H. Kruse, B. V. Jacak, and H. Stöcker, Phys. Rev. Lett. **54**, 289 (1985).

[10] J. Aichelin, Phys. Rep. (in press).

[11] C. Gale, G. Bertsch, and S. Das Gupta, Phys. Rev. C **35**, 1666 (1987); C. Gale, *ibid.* **36**, 2152 (1987); J. Aichelin, A. Rosenhauer, G. Peilert, H. Stöcker, and W. Greiner, Phys. Rev. Lett. **58**, 1926 (1987).

[12] J. Gosset, O. Valette, J. P. Alard, J. Augerat, R. Babinet, N. Bastid, F. Brochard, N. De Marco, P. Dupieux, Z. Fodor, L. Fraysse, P. Gorodetzky, M. C. Lemaire, D. L'Hôte, B. Lucas, J. Marroncle, G. Montarou, M. J. Parizet, J. Poitou, C. Racca, A. Rahmani, W. Schimmerling, and Y. Terrien, Phys. Rev. Lett. **62**, 1251 (1989).

[13] R. Brockmann, J. W. Harris, A. Sandoval, R. Stock, H.

Ströbele, G. Odyniec, H. G. Paugh, L. S. Schroeder, R. E. Renfordt, D. Schall, D. Bangert, W. Rauch, and K. L. Wolf, Phys. Rev. Lett. **53**, 2012 (1984).

[14] C. Hartnack, H. Stöcker, and W. Greiner, in Proceedings of the International Workshop on Gross Properties of Nuclei and Nuclear Excitations XVI, Hirschegg, Austria, edited by H. Feldmeier, GSI Report, ISSN 0720-8715, 1988, p. 138.

[15] G. Odyniec, J. Bartke, S. I. Chase, J. W. Harris, H. G. Pugh, G. Rai, W. Rauch, L. S. Schroeder, L. Teitelbaum, M. Tincknell, R. Stock, R. Renfordt, R. Brockmann, A. Sandoval, H. Ströbele, K. L. Wolf, and J. P. Sullivan, in Proceedings of the 8th High Energy Heavy Ion Study, Berkeley, edited by J. Harris and G. Wozniak, LBL Report 24580, 1988, p. 215.

[16] S. I. Chase, P. Barnes, J. W. Harris, J. Miller, G. Odyniec, W. Rauch, L. Teitelbaum, S. Tonse, R. E. Renfordt, and M. L. Tincknell, in Proceedings of the Workshop on Nuclear Dynamics VI, Jackson Hole Wyoming, edited by J. Randrup, LBL Report 28709, 1990, p. 67.

[17] D. Hahn and N. K. Glendenning, Phys. Rev. C **37**, 1053 (1988).

[18] B. A. Li and W. Bauer, Phys. Lett. B **254**, 335 (1991).

[19] J. W. Harris, NA35 collaboration, Nucl. Phys. **A498**, 133 (1989); J. Schukraft, Helios collaboration, *ibid.* **A498**, 79 (1989); T. W. Atwater, P. S. Freier, and J. I. Kapusta, Phys. Lett. B **199**, 30 (1987).

[20] E. V. Shuryak, Phys. Lett. B **207**, 345 (1988); Phys. Rev. D **42**, 1764 (1990).

[21] K. S. Lee and U. Heinz, Z. Phys. C **43**, 425 (1989).

[22] D. Kusnezov and G. F. Bertsch, Phys. Rev. C **40**, 2075 (1989).

[23] M. Kataja and P. V. Ruuskanen, Phys. Lett. B **243**, 181 (1990).

[24] G. E. Brown, J. Stachel, and G. M. Welke, Phys. Lett. B **253**, 19 (1991).

[25] N. Porile *et al.*, in Proceedings of the Seventh Winter Workshop on Nuclear Dynamics, edited by J. Kapusta and W. Bauer (World Scientific, Singapore, to be published).

[26] C. M. Ko, Q. Li, and R. Wang, Phys. Rev. Lett. **59**, 1084 (1987); C. M. Ko and Q. Li, Phys. Rev. C **37**, 2270 (1988).

[27] B. Blättel, V. Koch, W. Cassing, and U. Mosel, Phys. Rev. C **38**, 1767 (1988).

[28] J. Aichelin, Phys. Lett. **164B**, 261 (1985).

[29] S. J. Wang, B. A. Li, W. Bauer, and J. Randrup, Ann. Phys. (N.Y.) (in press).

[30] A. B. Migdal, Rev. Mod. Phys. **50**, 107 (1978); B. Friedman, V. R. Pandharipande, and O. N. Usmani, Nucl. Phys. **A372**, 483 (1981); G. F. Bertsch, G. E. Brown, V. Koch, and B. A. Li, *ibid.* **A490**, 745 (1988).

[31] W. Cassing, K. Niita, and S. J. Wang, Z. Phys. A **331**, 439 (1988).

[32] S. J. Wang and W. Cassing, Nucl. Phys. **A495**, 371c (1989).

[33] W. Cassing and S. J. Wang, Z. Phys. A **337**, 1 (1990).

[34] W. Cassing and U. Mosel, Prog. Nucl. Phys. **25**, 235 (1990).

[35] J. N. Ginocchio, Phys. Rev. C **17**, 195 (1978).

[36] P. J. Siemens, in Proceedings of 8th High-Energy Heavy-Ion Study, Berkeley, edited by J. Harris and G. Wozniak, LBL Report 24580, 1988, p. 511.

[37] P. J. Siemens, M. Soyeur, G. D. White, L. J. Lantto, and K. T. R. Davis, Phys. Rev. C **40**, 2641 (1989).

[38] J. Randrup, Nucl. Phys. **A314**, 429 (1979).

[39] J. Cugnon, T. Mizutani, and J. Vandermeulen, Nucl. Phys. **A352**, 505 (1981); J. Cugnon, D. Kinet, and J. Vandermeulen, *ibid.* **A379**, 553 (1982).

[40] J. Cugnon and M. C. Lemaire, Nucl. Phys. **A489**, 781 (1988).

[41] J. J. Molitoris, H. Söcker, and B. L. Winer, Phys. Rev. C **36**, 220 (1987).

[42] C. Y. Wong, Phys. Rev. C **25**, 1460 (1982).

[43] Gy. Wolf, G. Batko, W. Cassing, U. Mosel, K. Niita, and M. Schäfer, in *Proceedings of Corinnes (Nantes, 1990)*, edited by D. Ardouin (World Scientific, Singapore, 1990); Gy. Wolf, G. Batko, W. Cassing, and U. Mosel, Nucl. Phys. **A517**, 615 (1990).

[44] B. J. VerWest and R. A. Arndt, Phys. Rev. C **25**, 1979 (1982).

[45] Y. Kitazoe, M. Sano, H. Toki, and S. Nagamiya, Phys. Lett. **166B**, 35 (1986).

[46] Particle Data Group, Phys. Lett. B **204**, 1 (1988).

[47] W. Bauer, MSUCL Report-699.

[48] H. J. Pirner and B. Schurmann, Nucl. Phys. **A316**, 461 (1979).

[49] H. W. Barz, B. Lukács, J. Zimányi, G. Fái, and B. Jakobsson, Z. Phys. A **302**, 73 (1981).

[50] H. Oeschler *et al.*, KAOS proposal to the Program Advisory Committee of the Gesellschaft für Schwerionenforschung, 1989.

[51] W. Bauer, Phys. Rev. Lett. **61**, 2534 (1988).